Electronic Supplementary Material (ESI) for Journal of Materials Chemistry A.

Electronic Supplementary Information

Manipulation of n → π^* electronic transitions via implanting thiophene rings into two-dimensional carbon nitride nanosheets for efficient photocatalytic water purification

Fengting He[a], Xiaoming Liu[a], Xiaoli Zhao[c], Jinqiang Zhang[d], Pei Dong[a], Yang Zhang[a], Chaocheng Zhao[a,*], Hongqi Sun[c], Xiaoguang Duan[d*], Shaobin Wang[d], and Shuaijun Wang[b*]

[a] *State Key Laboratory of Petroleum Pollution Control, China University of Petroleum (East China), 66 West Changjiang Road, Qingdao 266580, PR China*
[b] *School of Energy and Power Engineering, Jiangsu University, Zhenjiang 212013, PR China*
[c] *School of Engineering, Edith Cowan University, 270 Joondalup Drive, Joondalup, WA 6027, Australia*
[d] *School of Chemical Engineering and Advanced Materials, The University of Adelaide, North Terrace, Adelaide, SA 5005, Australia*

*Corresponding Authors.
E-mail: zhaochch@upc.edu.cn(C. Zhao); xiaoguang.duan@adelaide.edu.au (X. Duan); shuaijunwang@ujs.edu.cn (S. Wang)

Contents

TEXT S1. Characterization

The transmission electron microscopy (TEM, TALOS F200), scanning electron microscope (SEM, S4800) and atomic force microscopy (AFM, CSPM5500LS) was performed to observe the morphology. The crystal structures of the samples were evaluated by X-ray diffraction (XRD, Bruker D8), Solid-state ^{13}C NMR spectra (Bruker ADVANCEIII), and the Fourier transforms infrared (FTIR, Nicolet Nexus 670) spectra. The nitrogen adsorption-desorption isotherms were determined on a Micromeritics sorption analyzer (ASAP 2010). X-ray photoelectron spectroscopy (XPS, ESCALAB 250xi) studies were conducted to analyze the surface chemical element. The diffuse reflectance spectra (DRS) were collected on UV–visible spectrophotometer (TU-1901). Photoluminescence (PL, F-4600) was used to analyze the electron-hole separation efficiency of materials. The electron spin resonance (ESR) spectroscopy was obtained using a Bruker A300 spectrometer.

The photoelectric performance of the sample was tested on the CHI-660B electrochemical workstation (China). 5 mg of the catalyst was dispersed in 250 μL of deionized water, and then 20 μL of Nafion solution was added to coat the mixture evenly on the FTO conductive glass. The catalyst/FTO, saturated calomel electrode, and platinum sheet were used as working electrodes, reference electrodes, and counter electrodes, respectively. The electrodes were immersed in Na_2SO_4 electrolytic solution. Electrochemical impedance (EIS) and transient photocurrent (IT) were performed under stable open-circuit voltage conditions.

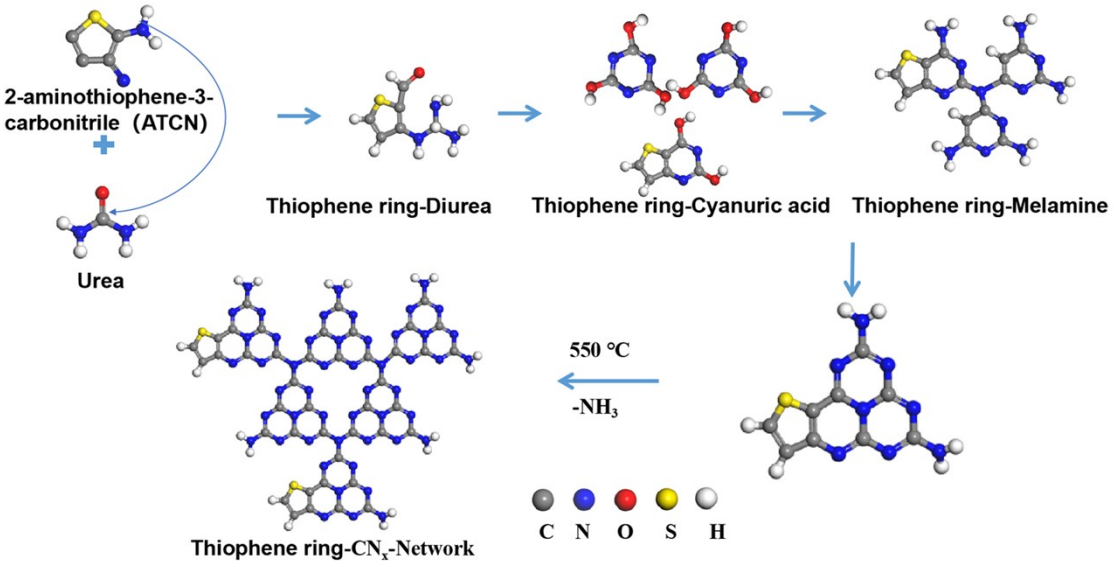

Fig. S1. The copolymerization of urea with ATCN

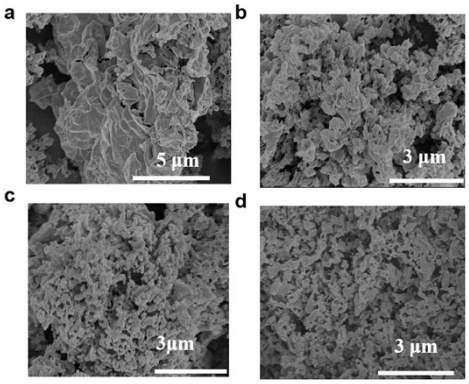

Fig. S2. SEM images of (a)C_3N_4, (b)2D CNNS, (c) 0.10%-Th_{ing}-CN, and (d) 2D Th_{ing}-CNNS.

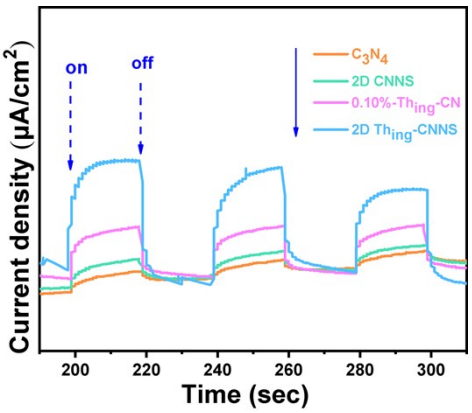

Fig. S3. The I-T spectra of C_3N_4, 2D CNNS, 0.10%- Th_{ing} -CN, and 2D Th_{ing} -CNNS

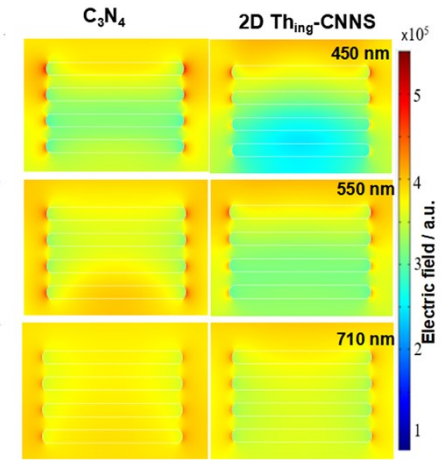

Fig. S4. The FEM results of near electric field distribution for C_3N_4 and 2D Th_{ing}-CNNS, under the radiation with the wavelength of (a) 450 nm, (b) 550 nm, and (c) 710 nm radiation, at the incident angle of 0°.

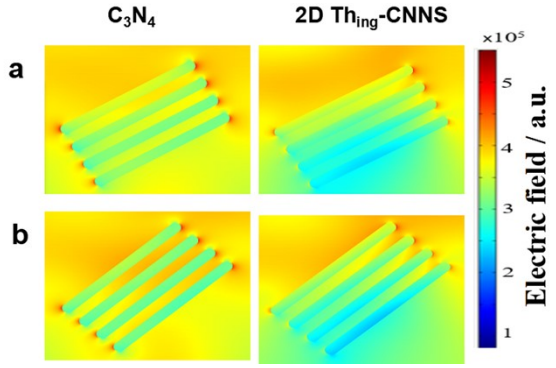

Fig. S5. The FEM results of near electric field distribution for C_3N_4 and 2D Th_{ing}-CNNS, under 450 nm radiation, at the incident angle of (a) 30°, and(b) 45°.

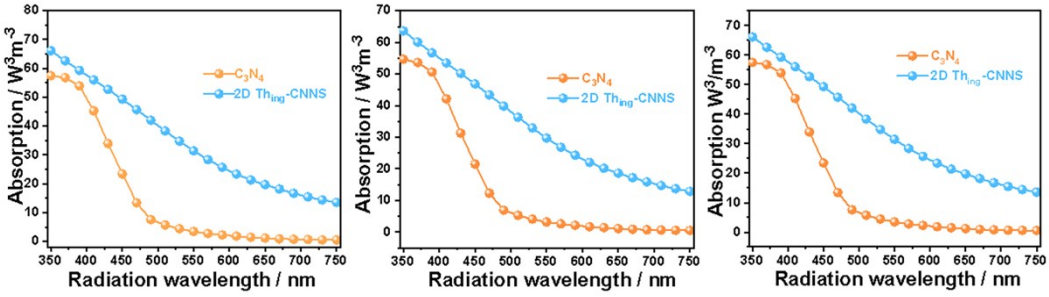

Fig. S6. The FEM results of near electric field distribution on C_3N_4 and 2D Th_{ing}-CNNS under the radiation of wavelength 350 nm, at the incident angle of (a) 30°, and (b) 45°.

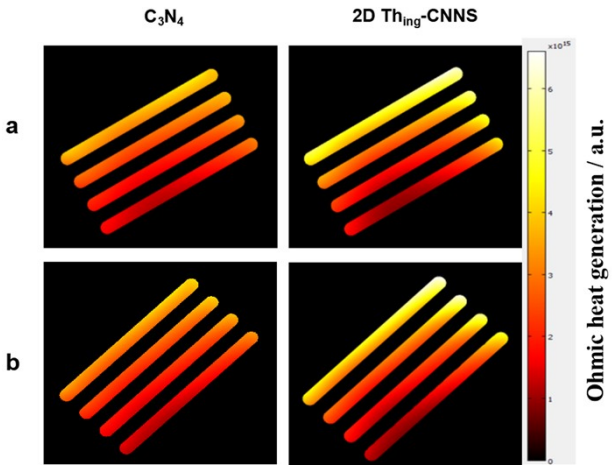

Fig. S7. The FEM results of Ohmic heat generation by C_3N_4 and 2D Th_{ing}-CNNS, under the radiation of wavelength 350 nm, and at the incident angle of (a) 30°, and (b) 45°.

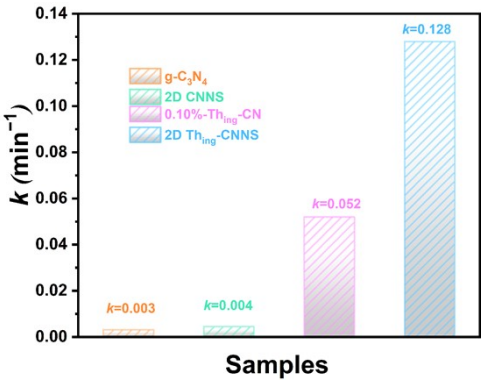

Fig. S8. The first-order kinetic constant *k* of C_3N_4, 2D CNNS, 0.10%-Th_{ing}-CN, and 2D Th_{ing}-CNNS

Table S1. Yield of the prepared samples

Samples	**Ultimate yield（%）**
C_3N_4	3.51
2D CNNS	2.50
0.1%-Th_{ing}-CN	4.13
2D Th_{ing}-CNNS	3.05

Table S2. Textural properties of the prepared samples

Samples	S_{BET} ($m^2 g^{-1}$)	Pore size (nm)	Pore volume ($cm^3 g^{-1}$)
C_3N_4	41.6	0.14	13.70
2D CNNS	76.4	0.29	14.86
0.10%-Th_{ing}-CN	40.7	0.12	12.14
2D Th_{ing}-CNNS	82.2	0.37	17.56

Table S3. Elemental analysis of the prepared samples

	C	N	C/N	O	S
C_3N_4	34.47	60.52	0.562	3.24	-
2D CNNS	33.81	59.59	0.567	4.24	-
0.05%-Th_{ing}-CN	34.09	60.24	0.566	3.26	<0.1
0.10%-Th_{ing}-CN	34.24	60.07	0.570	3.39	0.11
0.30%-Th_{ing}-CN	34.31	59.76	0.573	3.60	0.23
1.00%-Th_{ing}-CN	36.18	53.32	0.678	6.50	1.02
2D Th_{ing}-CNNS	33.83	59.02	0.573	4.70	0.09

Table S4. The peak-area ratio between C-N=C and N-$(C)_3$ of the prepared samples

Samples	C-N=C/C-$(N)_3$
C_3N_4	5.48
2D CNNS	5.28
0.1%-Th_{ing}-CN	5.23
2D Th_{ing}-CNNS	5.03

Table S5. Summary of time-resolved photoluminescence data for catalyst preparation

Samples	A1	τ1	A2	τ2	τ
C_3N_4	852.13	7.57	2111.56	1.18	5.80
2D CNNS	2179.96	1.40	783.29	10.99	8.49
0.10%-Th_{ing}-CN	2377.33	1.13	675.16	4.73	3.09
2D Th_{ing}-CNNS	954.41	3.93	2058.60	0.94	2.92